

# Precise Hybrid Method for Solving the Selectivity Problem of Overcurrent Relays Due to PV Uncertainty

Faeze Mohajer<sup>1</sup>, Hossein Kazemi Kargar<sup>\*1</sup>, Ahmad Salemnia<sup>1</sup>, Javad Sadeh<sup>2</sup>

<sup>1</sup>Electrical Engineering Faculty, Shahid Beheshti University, Tehran, Iran

<sup>2</sup>Electrical Engineering Faculty, Ferdowsi University of Mashhad, Mashhad, Iran

## ARTICLE INFO

## ABSTRACT

### Article history:

Received: 27 June 2024

Revised: 13 October 2024

Accepted: 17 November 2024

### Keywords:

Overcurrent relay  
Setting group  
Photovoltaic  
Uncertainty  
K-medoids  
Interval linear programming

Photovoltaic (PV) power plants include several parallel and series units. PV uncertainty due to scheduled or forced outages of these units affects the coordination of overcurrent relays (OCRs) and may violate the optimization constraint. This paper proposes a novel hybrid method to solve the selectivity problem of overcurrent relays due to photovoltaic power plant uncertainty. The proposed technique exploits K-medoids and interval linear programming (ILP) to provide setting groups (SGs). The recommended method not only maintains relay coordination for all PV generation scenarios, but also optimizes their operating time. In addition, this method can also be applied to the uncertainties caused by the synchronous distribution generation (DG) unit, which is verified in the studied networks. This research has been tested on the IEEE 8-bus and IEEE 30-bus distribution systems and the superiority of the proposed method in solving the selectivity problem and relay trip time optimization is demonstrated by the simulation results.



Copyright: © 2024 by the authors. Submitted for possible open access publication under the terms and conditions of the Creative Commons Attribution (CC BY) license (<https://creativecommons.org/licenses/by/4.0/>)

## 1. Introduction

Overcurrent relays play a key role in the protection of the distribution system, and their coordination is necessary for selective and speedy protection. Changes in the generation level and outage of distributed generations such as PVs may change the short circuit current. This uncertainty which occurs due to the sudden (failure) or scheduled (for maintenance purposes) outage of series and parallel PV units may miscoordinate the protection scheme. Therefore, the coordination of overcurrent relays with the aim of reducing or eliminating the effect of uncertainties due to changes in the production level of PVs has been investigated in the literature.


Overcurrent relay coordination methods considering uncertainties can be divided into robust and adaptive techniques. In the robust methods, there is a constant setting

for all considered uncertainties which increases the operating time of the relays. Adaptive methods identify changes in the network and then apply the appropriate settings to the relays [1].

As examples of robust techniques, the uncertainty of line outage is considered in the OCR coordination problem in [2, 3]. Genetic algorithm (GA) and linear programming (LP) are used by Noghabi, et al. to solve this problem [2] which provide a robust setting for overcurrent relays similar to [4]. Noghabi, et al. employed the interval linear programming (ILP) method to solve it [3]. Amraee formulated the OCR coordination problem as a mixed integer nonlinear programming (MINLP), solved by seeker optimization technique [5]. An inverse piecewise constant characteristic for OCRs has been presented in [6] by stochastic mixed-integer linear programming. Further,

\* Corresponding author

E-mail address: [h\\_kazemi@sbu.ac.ir](mailto:h_kazemi@sbu.ac.ir)

 <https://orcid.org/0000-0001-7392-3453>

<http://dx.doi.org/10.48308/ijrtei.2024.236129.1049>

Monte Carlo simulation has been used to calculate the probability of a fault current observed by the relay. The dynamic model of OCR is used by Ghotbi, et al. to consider the transient short-circuit current of wind farms and the OCR coordination problem is formulated as a binary linear programming (BLP) [7]. In [3, 4] and [8], the relays are coordinated in proportion to the DGs' capacity rise which has been predicted. Uncertainties in the line parameters and current transformer ratios are estimated by Monte Carlo simulation in [9]. In this research, the authors suggested ILP to solve the coordination problem. Shabani and Karimi provided a robust setting by considering the uncertainties of changes in operation conditions, changes in fault conditions, errors in measuring equipment, and DG outages [10]. A multi-function scheme for phase and ground faults with standard and non-standard tripping characteristics is formulated in [11]. This approach takes into account the different operating conditions (with and without PV).

Adaptive methods for overcurrent relay coordination have also been considered in several existing studies. In [12-14], DG on/off modes have been defined and according to the DG operating mode, a certain number of settings have been calculated and stored in the relay. As the number of DGs increases, the number of these settings rises, burdening the computation process. A hardware-in-the-loop adaptive protection scheme has been presented by Papaspiliotopoulos, et al. to coordinate the overcurrent relays [14]. According to the changes in the DGs' generation, Purwar, et al. have considered outage, maximum, and minimum DG generation [15]. Proposed adaptive protection using telecommunication systems and numerical relay capability is applicable to radial networks and mesh systems with different DG connection modes and sizes. A comparison of this method with [2] and [16] indicates that it has provided a faster and more robust performance in a network with various operating modes. In [17], the K-means clustering algorithm has been applied to classify different network structures. GA is utilized in [18] to classify the scenarios of the network topology change into a limited number of SGs. Moreover, the LP algorithm coordinates the OCRs within the SGs. The change of network structure and DG outage has been considered in [19, 20] and the SGs are presented. OCRs in each setting group are coordinated by MILP in [19] and the communication path between the central protection unit (CPU) and the protection devices has been fulfilled according to the IEC61850 standard. The multi-agent protection proposed in [20] is designed so that each agent can detect and isolate different faults in different operating modes of DG and network topology.

Adaptive methods in [21-24] have been presented using communication systems that ensure optimum settings of the protection systems with important changes in the network. Using this real-time setting, the optimum setting has been applied to the relays at any time [21]. The proposed method in [23] is only applicable to radial networks; hence, an adaptive method has been presented in [25] for mesh networks. Further, the recommended technique takes the uncertainty of the inverter and synchronous-based DGs into account. In [24], Purwar, et al. adopted a Center of Protection and Control (CPC) scheme, providing suitable actions to disconnect the faulty part of the system. Torshizi, et al. recommended the

measurement of the voltage and current of the relay(s) [26]. The presented analysis endorsed the promising performance of the presented scheme in radial, ring, and mesh configurations.

Photovoltaic power plants include several parallel and series units with string/commercial inverters. Outage of photovoltaic units and inverters are cause of changing the output of PVs [27, 28]. These outages can be emergency (such as component failure) or planned (such as a maintenance schedule) [29]. Changes in the PV outputs significantly affect the accuracy of the protection system. Partial or complete disconnection of PV units could cause the OCRs miscoordination. Accordingly, proposing a new optimal OCR coordination taking the PV system's uncertainty is a state-of-the-art topic. In this regard, this paper proposes a hybrid technique where the K-medoids algorithm first classifies the scenarios into a limited number of SGs. Afterward, the ILP algorithm coordinates the OCRs within the SGs optimally. In addition to maintaining the coordination of the OCRs under different scenarios, the proposed method reduces the operating time of the relays.

## 2. Overcurrent relay coordination

Different characteristics are defined for the operating time of overcurrent relays. The OCR operating time is a function of the current passing through the relay, its pickup current, and the time multiplier setting (TMS). This work uses the IEC standard modeling, defined as (1).

$$t_i = \frac{0.14}{\left(\frac{I_{f_i}}{I_{set_i}}\right)^{0.2} - 1} \times TMS_i = c_i(I_{f_i}, I_{set_i}) \times TMS_i \quad (1)$$

where,  $t_i$  and  $I_{f_i}$  are operating time and fault current passing through the relay  $i$ , respectively. Further,  $I_{set_i}$  and  $TMS_i$  are the pickup current and time multiplier setting of the relay  $i$ , respectively.

In the overcurrent relay coordination problem, two parameters of pickup current and  $TMS$  must be determined. Therefore, the overcurrent relay coordination is an optimization problem whose objective function includes minimizing the OCRs operating time. The optimization includes selectivity constraints as in equations (3) and (4). Using (1) for the relay operating times, the selectivity constraint of (3) becomes (5).

$$\text{minimize:} \quad J = \sum_{i=1}^N t_i = \sum_{i=1}^N c_i \times TMS_i \quad (2)$$

$$t_j - t_i \geq CTI \quad \forall (i,j) \in \Omega \quad (3)$$

$$TMS_i^{min} \leq TMS_i \leq TMS_i^{max} \quad (4)$$

$$c_j \times TMS_j - c_i \times TMS_i \geq CTI \quad \forall (i,j) \in \Omega \quad (5)$$

In the above equations,  $N$  is the total number of relays and  $\Omega$  is the total of the main and backup relay pairs. In addition,  $t_i$  and  $t_j$  are trip times of the main relay  $i$  and the backup relay  $j$ , respectively for the maximum short-circuit fault next to the main relay  $i$ . Furthermore,  $CTI$  stands for the coordination time interval between relay pairs, i.e., the minimum time that if the main relay does not operate, the backup relay should operate after it.  $TMS_i^{min}$  and  $TMS_i^{max}$

are the lower and upper bounds of  $TMS$  of the relay  $i$ , respectively. This coordination problem can be expressed as linear programming as (6a) to (6c) by replacing the  $TMS_i$  by  $x_i$ .

$$\text{minimize: } J = C^T X \tag{6a}$$

$$\text{Subject to: } AX \leq b \tag{6b}$$

$$x_i^{min} \leq x_i \leq x_i^{max} \quad i = 1.2 \dots N \tag{6c}$$

where,  $C$  and  $X$  are  $N \times 1$  vectors.  $X$  consists of  $x_i$  that are related to  $TMS_i$ .  $A$  is also an  $m \times N$  matrix, that  $m$  is the number of coordination constraints. Finally,  $b$  represents an  $N \times 1$  vector, consisting of  $CTI$ .

In general, there are different methods for modeling and solving the coordination problem of OCRs such as linear and nonlinear modeling methods, integer and mixed-integer programming, and ILP. The ILP method is very widely used in the presence of uncertainties where the coefficients of objective function and constraints, limited to an interval, have different sets.

Change in size or complete outage of PVs cause the OCRs miscoordination by changing the fault current. In general, miscoordination in a network occurs in a situation where the DG is located between the main and backup relays. Primary and backup relays that have been coordinated traditionally for maximum DG outputs by the CTI, as the unit number of the PV decreases, the main relay fault current also reduces. Therefore, the time interval between the main and backup relays becomes less than CTI and causes the OCRs miscoordination. In the following sections, a hybrid solution is presented to solve the OCRs coordination problem in such cases, i.e., in the presence of PV power plants.

### 3. K-medoids clustering algorithm

A cluster is a collection of data with similar properties and different properties from the components of other clusters. Fig. 1 shows the K-medoids clustering algorithm, where the number of clusters assumed is known a priori. In the first step, the initial center of the cluster is randomly determined and then the data are categorized according to the distance from the center of the cluster. The center of the cluster is recalculated again using the minimum distance of data and the data of each cluster is specified again. This algorithm is repeated until the cluster centers remain constant in two consecutive iterations of the algorithm.

### 4. Proposed combined method of k-medoids and ILP

Most overcurrent relay coordination methods consider the maximum DG capacity. The emergency or planned partial or complete outage of a PV power plant leads to a change in the fault current level and OCRs miscoordination. The method proposed in this paper considers the uncertainty caused by the change in the PV generation size in the coordination of overcurrent relays. The proposed method has two steps. In the first step, the K-medoids clustering algorithm determines the clusters and their corresponding PV generation size. In the second step, the ILP algorithm optimally coordinates the overcurrent relays.

**Stage 1:** It is hypothesized that the OCRs are numerical and have the ability to store several setting groups which are applied to relays using the IEC 61850 standard [30]. Combinations of PV generation levels are placed in each

cluster in which the scenarios have the same values of the sensitive constraints (SCs). In the proposed technique, the sensitive constraints must be defined at first. Therefore, the constraints related to the primary and backup relay pairs in which the PV power plants are placed between them, are called sensitive constraints. Equation (7) shows the SC formula for  $i$  and  $j$  main and backup relays pair. Then, SC must be calculated for all PV generation levels. For a network with  $q$  PV power plants, the total number of PVs generation scenarios ( $n_t$ ) is calculated by (8) and the SC values must be calculated for them.  $nu_q$  is the total number of units for the  $q$ -th PV power plant. For example, for a network consists of a 5MW and a 3MW PVs while each source composed of 1MW units, by considering the possibility of 0MW for each PVs, there are  $6 \times 4 = 24$  scenarios.

$$SC = t_j - t_i - CTI \tag{7}$$

$$n_t = (nu_1 + 1) \times \dots \times (nu_q + 1) \tag{8}$$

Therefore, the following steps are performed in this stage:

- 1) Coordination of overcurrent relays by considering the maximum power output ( $P_{max\_i}$ ) for all PV power plants (conventional method).
- 2) Calculation of SC matrix according to (9). Matrix SC is  $n_t \times p$ , that  $n_t$  stands for all PVs generation states and  $p$  is the number of sensitive constraints in the network.
- 3) Classification of the different PVs generation states using the K-medoids clustering algorithm based on the determined SC values.

$$SC = \begin{bmatrix} SC(1,1) & \dots & SC(1,p) \\ \vdots & \ddots & \vdots \\ SC(n_t,1) & \dots & SC(n_t,p) \end{bmatrix} \tag{9}$$

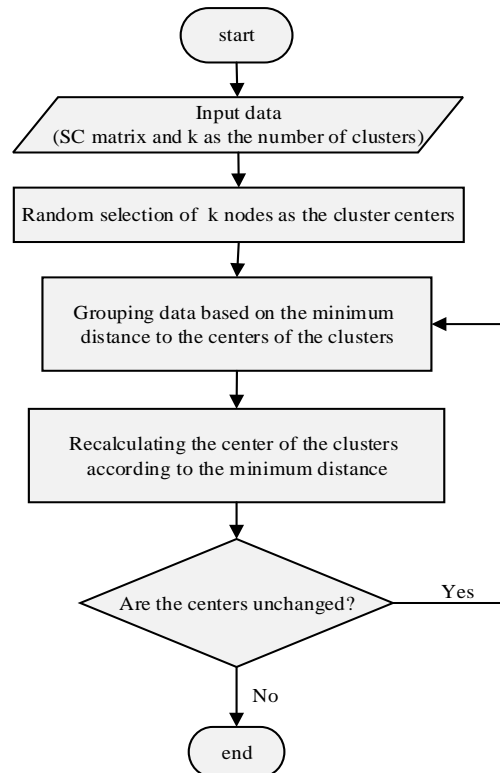


Fig. 1. Flowchart of the K-medoids clustering algorithm

**Stage 2:** After determining the clusters, the setting groups for each cluster must be provided. In each cluster, there are different PV generation levels, which can be defined as the interval output of PV power ( $P_{pv_q}^I$ ). According to (10), the maximum fault current of the relays in each cluster is a function of the size of the photovoltaic power plants.

$$I_f^I = h(P_{pv_1}^I, P_{pv_2}^I, \dots, P_{pv_q}^I) \quad (10)$$

where,  $I_f^I$  is the interval fault current passing through the overcurrent relay. Therefore, the maximum fault current of the relays in each cluster has different values inside a limited interval between a minimum and a maximum set. In the same way, the coefficient of the operating time of the relay is expressed as an interval coefficient as (11). According to (12) the matrix  $C^I$  has an upper bound  $\bar{C}$  and a lower bound  $\underline{C}$ .

$$C^I = f(I_f^I, I_{set}) = f(h(P_{pv_1}^I, P_{pv_2}^I, \dots, P_{pv_q}^I), I_{set}) \quad (11)$$

$$C^I = [\bar{C} \quad \underline{C}] \quad (12)$$

Therefore, the coefficients of the objective function and the matrix of the coordination constraints in equations 5a to 5c are expressed as an interval matrix. The coordination problem is also formulated as an ILP problem in (13a) and (13b):

$$\text{minimize: } J = (C^I)^T X \quad (13a)$$

$$\text{Subject to: } A^I x \leq b \quad \forall (i,j) \in \Omega \quad (13b)$$

It is noticeable that the strong solution to the ILP problem with inequality constraints is obtained by solving the standard LP [31] as (14a) to (14d).

$$\text{minimize: } J = (\bar{C})^T X \quad \text{or} \quad J = (\underline{C})^T X \quad (14a)$$

$$\text{Subject to: } \bar{A}X_1 - \underline{A}X_2 \leq b \quad (14b)$$

$$X_1 \geq 0 \quad X_2 \geq 0 \quad (14c)$$

$$X = X_1 - X_2 \quad (14d)$$

The steps to coordinate OCRs in each cluster are described as follows:

- 1) Consideration of maximum DG generation and load flow to calculate relay load current and pickup current ( $I_{set_i} = 1.2I_{load_i}$ ).
- 2) Determination of the maximum fault current passing through the OCRs for all scenarios in each cluster for steps 3 and 4.
- 3) Calculation of the objective function coefficient matrix. It is worth mentioning that due to the linearity

of the coordination problem, the magnitude of the coefficients of the objective function has no effect on the result of the problem, i.e., there is no difference in using  $\bar{C}$  or  $\underline{C}$  in the problem modelling.

- 4) Calculation of  $\bar{A}$  and  $\underline{A}$  using the information of steps 1 and 2.
- 5) Solving the LP problem in Equation (14a) to (14d) for each cluster and calculation of the setting groups.

## 5. Simulation results

The proposed method has been evaluated on two test systems simulated with the DIGSILENT software. The first one is the IEEE 8-bus system consisting of two PV systems. To verify the correctness of the proposed method on a larger distribution network, the IEEE 30 bus system was selected, which has two PVs on buses and a synchronous DG. The short circuit currents passing through the relays for faults in front of them in scenarios with and without PVs, for both networks, are added in the Appendix.

The value of CTI in all of the coordination methods applied to the 8-bus network is 0.3 and for the 30-bus network is equal to 0.2 to check the performance of different methods and relay miscoordination with different values of CTI. The PV system block diagram is presented in Fig. 2. This model includes PV arrays, a DC bus, a capacitor, an active power reduction model for frequency increase conditions, a controller and static generator. The static generator block includes a DC/AC converter or inverter which is controlled by a voltage-oriented controller (VOC). The active power can be regulated by adjusting the current  $i_d$ , which is based on the DC voltage regulation of the PV system. Similarly, the reactive power can be controlled by adjusting the current  $i_q$ , which follows an AC voltage regulation strategy [32]. The proposed method for reactive power control in this paper adheres to the German network standards outlined in [33]. In this approach, power generation sources are required to compensate for voltage drops by injecting reactive current. Consequently, if voltage drop exceeds 10%, voltage control should be activated.

- The 8-bus standard system

The 8-bus standard system is simulated in the DIGSILENT platform. As shown in Fig. 3, the lines in this system are protected by 14 OCRs. When a fault initiates in the network, the PV feeds the fault current which depends on the inverter model. Similar to [34], the fault current injected by PV is limited to 1 to 2 times of rated current under various scenarios.

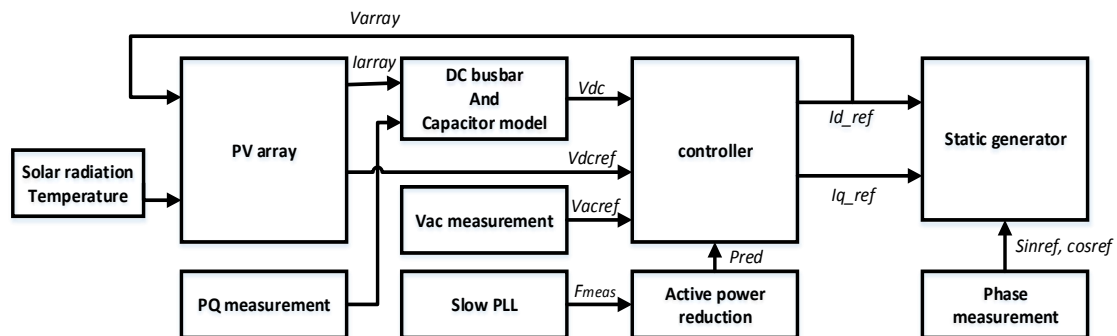


Fig. 2. Block diagram of PV system in DIGSILENT

The PV power plants include 9 parallel units with 1 MW capacity while the outage of any of the parallel units is possible. Hence, there are 10 generation levels for each PV, and the total number of scenarios is 10×10=100. In order to have a better comparison of the results of the 8-bus network, this problem has been solved with four different methods:

- Method 1. Solving the coordination problem by conventional method considering maximum capacity for PVs [35].
- Method 2. Proposed method: Considering the PVs uncertainties and presenting setting groups for OCRs by using the proposed combined method K-medoids and ILP.
- Method 4. Considering the PVs uncertainties and solving the coordination problem by ILP [3].
- Method 3. Considering the PVs uncertainties and presenting setting groups for OCRs by using the combined method of K-medoids and LP [36].

**Method 1:** The OCRs setting by conventional coordination is shown in Table I. It is worth mentioning that the breakpoints are determined according to reference [37] in methods 1 to 4.

**Method 2:** To coordinate OCRs by the proposed method, the value of the sensitive constraints should be initially calculated for all 100 scenarios, using OCRs setting of method 1. The sensitive constraints of the test system are shown in Table II and the SC matrix is a 100×4 matrix. For example, the PVs capacities for scenarios 91 to 100 and the SC values for these scenarios are shown in Table III and Fig. 4, respectively. As can be seen, in the traditional coordination method by changing the PV generation, the value of sensitive constraints becomes negative and causes the OCRs to miscoordination. Using SC matrix information and the K-medoids algorithm, the scenarios of each cluster are identified. The number of clusters is considered to be 4. The scenarios and PV capacity of each cluster are shown in Tables IV and V, respectively. The OCRs in each cluster are optimally coordinated by the ILP method and their setting is shown in Table VI.

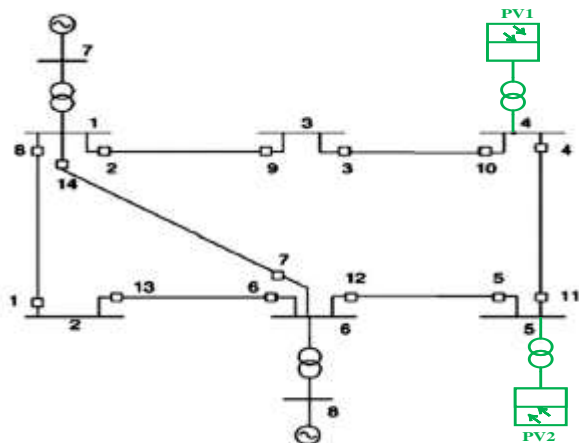


**Fig. 3.** 8-bus standard system with 2 photovoltaic power plant

In the relay coordination using the proposed method, by changing the size of PV power plants, the coordination constraints are not violated. Fig. 5 shows the values of the

sensitive constraints for scenarios 4 to 10 in cluster 1, which have positive values as the PV capacity changes.

**Method 3:** In this method, considering all scenarios (generation levels of PVs), the coordination problem is modeled as the interval linear program and a robust setting is provided for all scenarios by ILP. Table VII shows the OCRs setting for Method 3. According to Table VIII, considering  $P_{max}$  for PVs, the operating time of the overcurrent relays is calculated for the fault in front of the main relay using methods 2 and 3. A comparison of methods 2 and 3 shows that in the proposed method, the operating time of relays is reduced apropos of method 3.

**Table I.** OCRs setting (Method 1)

Relay number	TMS	Ip (kA)
1	0.067	0.27459
2	0.234	0.28227
3	0.155	0.27959
4	0.107	0.27459
5	0.050	0.27209
6	0.143	0.27709
7	0.160	0.27459
8	0.050	0.27459
9	0.050	0.28227
10	0.113	0.27959
11	0.196	0.27459
12	0.276	0.27209
13	0.069	0.27709
14	0.050	0.27459
OF	6.0016	

**Table II.** Sensitive constraint in 8-bus system

Backup Relay	Primary Relay	Sensitive Constraint
R4	R3	$SC_1 = t_4 - t_3 - CTI$
R5	R4	$SC_2 = t_5 - t_4 - CTI$
R11	R10	$SC_3 = t_{11} - t_{10} - CTI$
R12	R11	$SC_4 = t_{12} - t_{11} - CTI$

**Table III.** The capacity of PVs in scenarios 91 to 100

SC	91	92	93	94	95	96	97	98	99	100
PV1	9	8	7	6	5	4	3	2	1	0
PV2	0	0	0	0	0	0	0	0	0	0

**Table IV.** Scenario number of clusters obtained by K-medoids

Cluster1	Cluster2	Cluster3	Cluster4
4:10	51:53	54:60	1:3
15:20	61:64	65:70	11:14
26:30	71:75	76:80	21:25
37:40	81:86	87:90	31:36
48:50	91:97	98:100	41:47

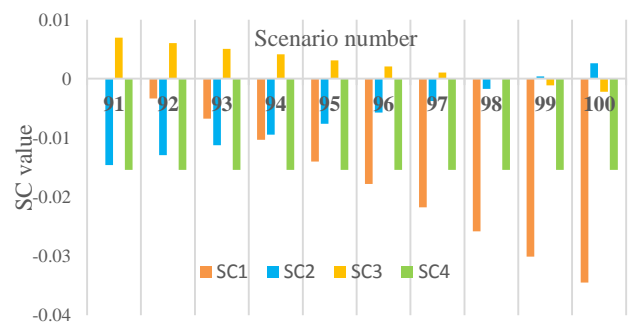


**Fig. 4.** SC values for scenarios 91 to 100 – OCRs coordination by Method 1

**Table V.** PVs capacity in each cluster

Cluster1		Cluster2		Cluster3		Cluster4	
PV1	PV2	PV1	PV2	PV1	PV2	PV1	PV2
3:9	0	0:2	5	3:9	5	0:2	0
4:9	1	0:3	6	4:9	6	0:3	1
5:9	2	0:4	7	5:9	7	0:4	2
6:9	3	0:5	8	6:9	8	0:5	3
7:9	4	0:6	9	7:9	9	0:6	4

**Table VI.** The OCRs setting for each cluster (Method 2)

Relay number	Ip (kA)	TMS (sec)			
		Cluster1	Cluster2	Cluster3	Cluster4
1	0.27459	0.067728	0.068547	0.069674	0.066576
2	0.28227	0.242242	0.241908	0.241032	0.243205
3	0.27959	0.162421	0.162002	0.161001	0.16351
4	0.27459	0.110616	0.108165	0.109149	0.109694
5	0.27209	0.05	0.05	0.05	0.05
6	0.27709	0.143435	0.144474	0.145927	0.14195
7	0.27459	0.162984	0.163632	0.164403	0.162215
8	0.27459	0.05	0.05	0.05	0.05
9	0.28227	0.05	0.05	0.05	0.05
10	0.27959	0.11355	0.11393	0.114489	0.11298
11	0.27459	0.198291	0.200401	0.200166	0.198534
12	0.27209	0.282265	0.282041	0.281807	0.282509
13	0.27709	0.069726	0.070171	0.070849	0.069039
14	0.27459	0.05	0.05	0.05	0.05
Objective Function		6.1800	6.1435	6.1287	6.1673

**Table VII.** The OCRs setting (Method 3)

Relay number	TMS (sec)	Ip (kA)
1	0.07098	0.27459
2	0.246134	0.28227
3	0.165358	0.27959
4	0.111569	0.27459
5	0.05	0.27209
6	0.148142	0.27709
7	0.167486	0.27459
8	0.05	0.27459
9	0.05	0.28227
10	0.116061	0.27959
11	0.203979	0.27459
12	0.287981	0.27209
13	0.072123	0.27709
14	0.05	0.27459
Objective Function	6.2364	

**Method 4:** In this method, the different scenarios are clustered using the K-medoids algorithm and the settings for each cluster are presented by linear programming. The scenarios and PV capacity of each cluster are the same as in method 2 (Tables IV and V). The setting groups of this method are illustrated in Table IX as well. Fig. 6 shows the values of the sensitive constraints for scenarios 4 to 10 in cluster 1. It is readily seen that the values of the sensitive constraints may be negative in some scenarios, i.e., some of the coordination constraints are violated.

In this section, three different coordination methods are investigated and compared with the proposed method. According to the results of the studies, by changing the size of the PV sources, in method 1 (conventional) and method 4 (K-medoids), coordination constraints have been violated. Further, in the method 3 which proposed a robust setting by the ILP method, the operating time of the relays increases in comparison with the proposed method. Therefore, the proposed combined method not only maintains the coordination of the relays under various PV

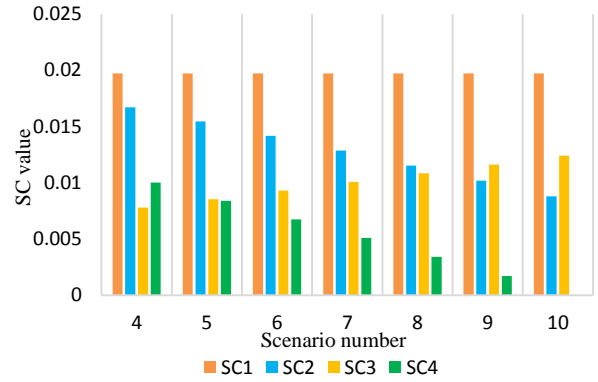


**Fig. 5.** SC values for scenarios 4 to 10 – OCRs coordination by Method 2 (proposed method)

**Table VIII.** Comparing the OCRs operating time of methods 2 and 3

Relay number	t (sec)	
	Method 1 (ILP)	Method 2 (SG3)
1	0.2802	0.2659
2	0.7296	0.7247
3	0.6168	0.6126
4	0.5652	0.5652
5	0.2400	0.2502
6	0.4411	0.4266
7	0.5322	0.5209
8	0.1487	0.1499
9	0.2420	0.2487
10	0.4087	0.4049
11	0.7257	0.7144
12	0.8450	0.8310
13	0.3012	0.2912
14	0.1598	0.1611
Sum	6.2364	6.1673

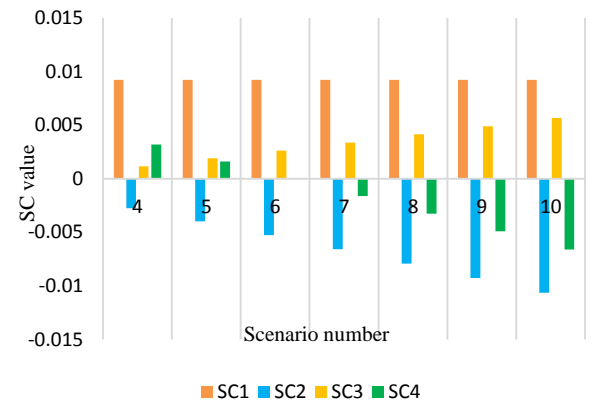


**Fig. 6.** SC values for scenarios 4 to 10 – OCRs coordination by Method 4

power plant generations but also the overall operating time of the relays increases slightly.

It is worth mentioning that in coordination methods 1 and 4, by considering any value for CTI, the coordination constraints would be violated by changing the level of PV generation. For CTI=0.2s for example, as the size of the PVs decreases, the time interval between the main and backup relay operation becomes smaller than 0.2s and the values of the sensitive constraints would be negative.

**Table IX.** The OCRs setting for each cluster (Method 4)

Relay number	Ip (kA)	TMS (sec)			
		Cluster1	Cluster2	Cluster3	Cluster4
1	0.27459	0.0648	0.066807	0.067976	0.064822
2	0.28227	0.2357	0.234739	0.234203	0.235711
3	0.27959	0.1569	0.155692	0.155021	0.156893
4	0.27459	0.1068	0.105513	0.106598	0.106776
5	0.27209	0.0500	0.05	0.05	0.05
6	0.27709	0.1392	0.141711	0.143205	0.139175
7	0.27459	0.1579	0.159481	0.160396	0.157943
8	0.27459	0.0500	0.05	0.05	0.05
9	0.28227	0.0500	0.05	0.05	0.05
10	0.27959	0.1111	0.112129	0.112738	0.111091
11	0.27459	0.1940	0.196027	0.195912	0.194004
12	0.27209	0.2761	0.275942	0.275829	0.276132
13	0.27709	0.0677	0.068899	0.069588	0.067737
14	0.27459	0.0500	0.05	0.05	0.05
Objective Function		6.0288	6.0113	6.0016	6.0288

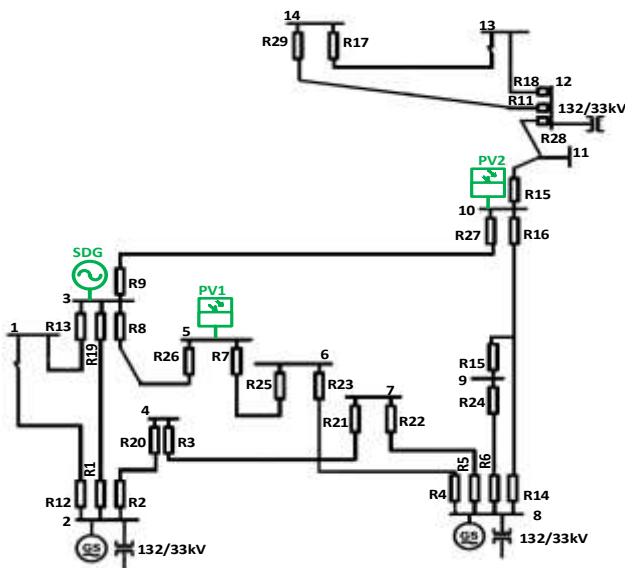


**Fig. 7:** The distribution portion of the IEEE 30-bus system

• IEEE 30-bus System

The single line diagram of the distribution network portion of the modified 30-bus IEEE standard network is shown in Fig. 7 which consists of 29 relays and 46 pairs of main and backup relays as shown in Table X. This network has two PVs on buses 5 and 10 and one synchronous DG on bus 3, so that the capacity of each DG is 10 MW (including 5 units of 2 MW). Relay settings for conventional (Method 1) and ILP (Method 4) coordination methods are shown in Table XI. The conventional method uses the LP to coordinate the relays for maximum DG capacity, and ILP considers all 2 MW unit outage scenarios of DGs for relay coordination. It should be noted that the value of CTI in all of the coordination methods applied to the 30-bus network is considered equal to 0.2 to clarify that in the conventional coordination method by any value of CTI, by changing the production units, the time interval between the main and backup relays performance will be reduced and coordination constraints will be violated.

For each DG, 6 production levels are considered with 2 MW steps, i.e. 10, 8, 6, 4, 2 and 0, which equals 216 (6 × 6 × 6) scenarios. The capacity of DGs for all scenarios is in Table XII. Using the conventional method settings of OCRs, the value of constraints was calculated for all scenarios and in some scenarios the SCVs for this network

are negative. The minimum value of the SCVs in different scenarios can be seen in Table XIII. This table also shows the SCVs when the relays are coordinated with CTI equal to 0.3 which can be seen with both CTI values, the sensitive constraints will be violated in some scenarios. Of course, choosing the CTI value will depend on the speed and accuracy of the networking equipment used. In this section, the CTI value is 0.2. Note that Table XIII lists only one of the scenarios in which the SCV has a minimum value and the minimum SCV occurred in similar scenarios for both CTI values. Fig. 8a shows sensitive constraints 15, 34, and 38 for different scenarios by conventional method coordination.

**Table X.** Pairs of main and backup relays for the IEEE 30-bus system

num	Primary	backup	num	Primary	backup
1	1	20	24	13	1
2	2	19	25	13	26
3	3	2	26	13	27
4	4	16	27	14	22
5	4	24	28	14	23
6	4	23	29	15	6
7	5	16	30	16	9
8	5	22	31	16	28
9	5	24	32	17	11
10	6	16	33	18	10
11	6	22	34	19	26
12	6	23	35	19	27
13	7	8	36	20	21
14	8	1	37	21	4
15	8	27	38	22	3
16	9	1	39	23	7
17	9	26	40	24	14
18	10	9	41	24	16
19	10	14	42	25	5
20	10	15	43	26	25
21	11	10	44	27	14
22	12	19	45	27	15
23	12	20	46	27	28

In order to apply the proposed method to the 30-bus network, the SC matrix was first calculated using equation (9), then, using the K-medoids method, all scenarios were classified into 4 groups so that clusters 1 through 4 contain 90, 24, 12, and 90 scenarios, respectively. It is assumed that the relay can store 4 setting groups. Table XIV shows the coordination results for each cluster using the proposed method and in Fig. 8, the SCV for the proposed and conventional methods are compared for scenarios 211 to 216. As it is clear from the results, in the proposed method, the values of SCs are positive for all scenarios, furthermore, according to Table XV, the minimum SCV in the proposed method has values greater than or equal to zero. The objective function in the conventional method (Method 1), ILP method (Method 3) and the proposed method are not the same, therefore the value of the objective function is not appropriate to compare the performance of the approaches, for this reason, in Table XVI, the tripping time of the relays for the fault in front of them has been calculated and compared for several scenarios. The scenarios are selected so that each is related to a setting group and Table XVII shows the capacity of the DGs for each of these scenarios. Based on the results in Table XVI, the total trip time in the ILP method is higher than the conventional method. In addition, in scenarios 76 and 141, the proposed method decreased total relay trip time compared to LP (conventional) and ILP methods.

Therefore, it can be concluded that in the proposed method, for setting group that has a smaller number of scenarios, not only the constraints are not violated, but also in the case of increasing the number of setting groups (in case of relay availability) and consequently reducing the number of scenarios in each cluster, the operation time of the relays will also decrease.

**Table XI.** Relay coordination results by LP and ILP method for the IEEE 30 bus system

Relay	$I_{set}$ (kA)	TMS (ka)	
		LP	ILP (Method 4)
R1	0.0521	0.5480	0.7597
R2	0.0813	0.4630	0.6257
R3	0.0770	0.3703	0.5104
R4	0.3289	0.4057	0.5167
R5	0.1591	0.4540	0.5961
R6	0.4470	0.2617	0.3377
R7	0.1057	0.3886	0.5260
R8	0.1052	0.4625	0.6452
R9	0.1355	0.3735	0.4766
R10	0.1701	0.1539	0.1564
R11	0.1950	0.0884	0.0891
R12	0.0986	0.0500	0.0500
R13	0.0772	0.0500	0.0500
R14	0.2060	0.2041	0.2713
R15	0.0993	0.4867	0.4867
R16	0.1079	0.3661	0.4662
R17	0.1025	0.0500	0.0500
R18	0.1716	0.0500	0.0500
R19	0.0521	0.5162	0.6890
R20	0.0813	0.4244	0.5660
R21	0.0770	0.5326	0.6922
R22	0.3289	0.1375	0.1761
R23	0.1590	0.2602	0.3313
R24	0.4000	0.0524	0.0667
R25	0.1057	0.4235	0.5754
R26	0.1052	0.3556	0.4822
R27	0.1355	0.3419	0.4739
R28	0.1701	0.2160	0.2757
R29	0.1951	0.0500	0.0500
<b>OF</b>		<b>17.799</b>	<b>23.2153</b>

**Table XII.** DG capacities in different scenarios for the IEEE 30-bus system

scenario	SDG	PV1	PV2	scenario	SDG	PV1	PV2
1:6	10,8,6,4,2,0	10	10	109:114	10,8,6,4,2,0	10	4
7:12	10,8,6,4,2,0	8	10	115:120	10,8,6,4,2,0	8	4
13:18	10,8,6,4,2,0	6	10	121:126	10,8,6,4,2,0	6	4
19:24	10,8,6,4,2,0	4	10	126:132	10,8,6,4,2,0	4	4
25:30	10,8,6,4,2,0	2	10	133:138	10,8,6,4,2,0	2	4
31:36	10,8,6,4,2,0	0	10	139:144	10,8,6,4,2,0	0	4
37:42	10,8,6,4,2,0	10	8	145:150	10,8,6,4,2,0	10	2
42:48	10,8,6,4,2,0	8	8	151:156	10,8,6,4,2,0	8	2
49:54	10,8,6,4,2,0	6	8	157:162	10,8,6,4,2,0	6	2
54:60	10,8,6,4,2,0	4	8	163:168	10,8,6,4,2,0	4	2
61:66	10,8,6,4,2,0	2	8	169:174	10,8,6,4,2,0	2	2
67:72	10,8,6,4,2,0	0	8	175:180	10,8,6,4,2,0	0	2
73:78	10,8,6,4,2,0	10	6	181:186	10,8,6,4,2,0	10	0
79:84	10,8,6,4,2,0	8	6	187:192	10,8,6,4,2,0	8	0
85:90	10,8,6,4,2,0	6	6	193:198	10,8,6,4,2,0	6	0
90:96	10,8,6,4,2,0	4	6	199:204	10,8,6,4,2,0	4	0
97:102	10,8,6,4,2,0	2	6	205:210	10,8,6,4,2,0	2	0
103:108	10,8,6,4,2,0	0	6	211:216	10,8,6,4,2,0	0	0

**Table XIII.** The minimum SCV of the IEEE 30-bus system

SC	Min SCV			SC	Min SCV		
	0.2	0.3	Scenario		0.2	0.3	scenario
13	-0.0377	-0.0566	31	34	-0.0473	-0.0710	6
14	-0.0463	-0.0695	36	35	-0.0312	-0.0467	36
15	-0.0461	-0.0691	6	38	-0.0461	-0.0692	36
31	-0.0264	-0.0395	36	43	-0.0417	-0.0626	31

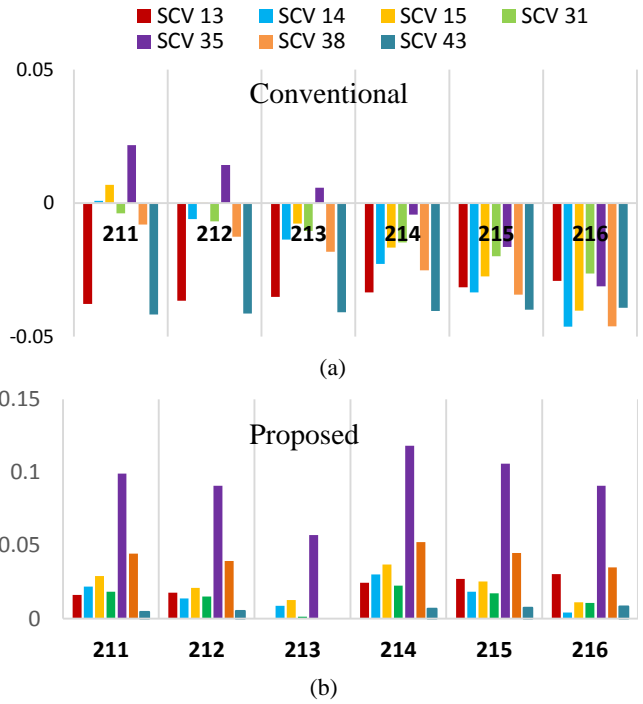


**Fig. 8:** SCVs for scenarios 211 to 216 (a) conventional method (b) proposed method

**Table XIV.** Relay settings using the proposed method for the IEEE 30-bus system

$I_{set}$ (kA)	TMS (sec)				
	Cluster 1	Cluster 2	Cluster 3	Cluster 4	
R1	0.0521	0.6218	0.565516	0.538682	0.64764
R2	0.0813	0.483795	0.445429	0.43001	0.530127
R3	0.0770	0.384597	0.353372	0.338875	0.428864
R4	0.3289	0.441638	0.412071	0.398225	0.45806
R5	0.1590	0.500062	0.460269	0.447314	0.519192
R6	0.4470	0.284713	0.265285	0.255082	0.297589
R7	0.1057	0.409795	0.382361	0.351328	0.456655
R8	0.1052	0.509246	0.46762	0.440757	0.555016
R9	0.1355	0.385271	0.36335	0.35006	0.420835
R10	0.1701	0.152724	0.152403	0.151777	0.155116
R11	0.1950	0.088066	0.088014	0.08784	0.088737
R12	0.0986	0.05	0.05	0.05	0.05
R13	0.0772	0.05	0.05	0.05	0.05
R14	0.2060	0.224287	0.20741	0.197921	0.235788
R15	0.0993	0.406658	0.374817	0.35896	0.422906
R16	0.1079	0.3815	0.360336	0.346834	0.413553
R17	0.1025	0.05	0.05	0.05	0.05
R18	0.1716	0.05	0.05	0.05	0.05
R19	0.0521	0.527649	0.490217	0.472544	0.586829
R20	0.0813	0.472306	0.434811	0.416342	0.490931
R21	0.0770	0.58757	0.544483	0.52469	0.607783
R22	0.3289	0.129925	0.126039	0.119512	0.154971
R23	0.1590	0.255406	0.246421	0.223273	0.293924
R24	0.4000	0.05	0.05	0.05	0.059204
R25	0.1057	0.473664	0.43106	0.416768	0.494186
R26	0.1052	0.385615	0.349938	0.331285	0.40633
R27	0.1355	0.387868	0.352759	0.335311	0.403986
R28	0.1701	0.231579	0.215846	0.209431	0.24338
R29	0.1951	0.05	0.05	0.05	0.05
<b>OF</b>		<b>18.9894</b>	<b>17.7047</b>	<b>16.9731</b>	<b>20.2897</b>

**Table XV.** Minimum SCVs comparison between proposed and conventional methods

SC	Min SCV		SC	Min SCV	
	conventional	proposed		conventional	proposed
13	-0.0377	0	34	-0.0473	0.0001
14	-0.0463	0	35	-0.0312	0.0512
15	-0.0461	0	38	-0.0461	0.0003
31	-0.0264	0.0004	43	-0.0417	0



**Table XVII.** Capacity of DGs for scenarios 216, 76, 141 and 1

Scenario	216			76		
	SDG	PV1	PV2	SDG	PV1	PV2
capacity	0	0	0	4	10	6
Scenario	141			1		
	SDG	PV1	PV2	SDG	PV1	PV2
capacity	6	0	4	10	10	10

**6. Conclusion**

In this paper, a new hybrid method is proposed to solve the selectivity problem of overcurrent relays due to the uncertainty of PV power plants. The presented method exploits the value of sensitive constraints to classify different generation scenarios by the K-medoids clustering algorithm. Then, optimal coordination for the scenarios of each cluster (setting groups) is found using interval linear programming. Therefore, by changing the PV generation levels, the relevant setting group is activated. The proposed method is applied to the IEEE 8-bus system with the presence of two 9MW PV power plants. To verify the correctness of the proposed method in larger networks, as well as against the uncertainty caused by the outage of synchronous DG units, this method was also applied to the 30-bus network, which includes two PV and one 10 MW synchronous DG. Also, to check the sensitivity of the different methods to the CTI value, the relays were coordinated in the 8-bus network

with a CTI value of 0.3 and in the 30-bus network with 0.2, then the results show that in the conventional method, the SCs are violated for both CTI values, but in the proposed method the coordination is done correctly. For example, in Scenario 1 in the setting Group 4, related to the IEEE 30-bus network, the total operating time of the relays for a fault in front of the relay in the proposed method has increased by two seconds compared to the conventional method. In contrast, in scenario 141 related to the setting Group 3, the total operation time of the relays for a fault in front of the main relay in the conventional method is 18.271 seconds, which has been reduced to 17.456 seconds in the proposed method. Meanwhile, the selectivity constraints are satisfied in all scenarios. Therefore, in some cases, the proposed method may lead to a negligible increase in the relay operation time, but in general, the results show that the proposed method has not only reduced the relay operation time in some clusters compared to the conventional method, but also satisfies all the constraints under different PV generation levels, different DG types, and different CTI values.

**Table XVI.** Comparison of relay trip time (sec) for three methods

Relay	Scenario 216 – SG1			Scenario 76 - SG2			Scenario 141 - SG3			Scenario 1- SG4		
	Method 1 [35]	Method 3 [36]	Proposed method	Method 1 [35]	Method 3 [36]	Proposed method	Method 1 [35]	Method 3 [36]	Proposed method	Method 1 [35]	Method 3 [36]	Proposed method
R1	0.9983	1.2196	0.8798	0.8695	1.2053	0.8973	0.8727	1.2097	0.8578	0.8644	1.1982	1.0215
R2	0.8674	1.1218	0.8301	0.8048	1.0875	0.7742	0.8086	1.0927	0.7509	0.7903	1.068	0.9049
R3	0.8028	1.0654	0.7729	0.7494	1.033	0.7151	0.753	1.038	0.6891	0.7364	1.0151	0.8529
R4	1.1158	1.3054	1.0249	0.9949	1.2671	1.0106	1.0055	1.2807	0.9871	0.9821	1.2508	1.1089
R5	0.9748	1.162	0.885	0.8715	1.1442	0.8835	0.873	1.1463	0.8601	0.863	1.1332	0.9869
R6	0.7996	0.9485	0.7351	0.7104	0.9166	0.72	0.7187	0.9272	0.7004	0.6997	0.9027	0.7955
R7	0.9571	1.2284	0.9077	0.842	1.1395	0.8284	0.8756	1.185	0.7915	0.824	1.1152	0.9682
R8	0.9818	1.2438	0.8917	0.8647	1.2061	0.8742	0.8591	1.1984	0.8187	0.8416	1.1739	1.0099
R9	0.8259	1.0217	0.8007	0.7606	0.9704	0.7398	0.7658	0.9771	0.7177	0.7379	0.9415	0.8314
R10	0.3405	0.3488	0.343	0.3322	0.3378	0.329	0.3346	0.3402	0.3301	0.3267	0.3322	0.3294
R11	0.2171	0.2195	0.218	0.2144	0.2159	0.2134	0.2152	0.2168	0.2138	0.2126	0.2141	0.2133
R12	-0.0891	0.0891	0.0891	0.087	0.087	0.087	0.0874	0.0874	0.0874	0.0858	0.0858	0.0858
R13	0.0852	0.0852	0.0852	0.0823	0.0823	0.0823	0.0828	0.0828	0.0828	0.0806	0.0806	0.0806
R14	0.4699	0.5685	0.4275	0.4162	0.5535	0.423	0.4199	0.5583	0.4072	0.4112	0.5467	0.4751
R15	0.8163	0.977	0.7348	0.719	0.9561	0.7363	0.7246	0.9634	0.7106	0.7122	0.947	0.8229
R16	0.8602	1.0511	0.8253	0.7965	1.0143	0.784	0.8008	1.0199	0.7588	0.7806	0.9941	0.8819
R17	0.1431	0.1431	0.1431	0.1415	0.1415	0.1415	0.1418	0.1418	0.1418	0.1407	0.1407	0.1407
R18	0.1177	0.1177	0.1177	0.1158	0.1158	0.1158	0.1162	0.1162	0.1162	0.1149	0.1149	0.1149
R19	0.9021	1.1781	0.8826	0.8399	1.121	0.7976	0.8457	1.1288	0.7741	0.8165	1.0898	0.9281
R20	0.9754	1.1688	0.8763	0.8602	1.1473	0.8814	0.866	1.155	0.8496	0.8532	1.138	0.9871
R21	1.0254	1.2081	0.9296	0.9128	1.1863	0.9331	0.9187	1.194	0.905	0.9055	1.1768	1.0333
R22	0.7603	1.0307	0.8044	0.7298	0.935	0.6691	0.7399	0.9479	0.6432	0.6928	0.8876	0.781
R23	0.8156	1.0581	0.8308	0.7507	0.956	0.711	0.7898	1.0059	0.6778	0.7296	0.9292	0.8243
R24	0.21	0.2803	0.2201	0.2075	0.2642	0.198	0.2102	0.2677	0.2006	0.2014	0.2565	0.2275
R25	0.9947	1.2084	0.8894	0.8796	1.1951	0.8953	0.8798	1.1954	0.8658	0.8727	1.1857	1.0183
R26	0.905	1.1316	0.8347	0.7851	1.0644	0.7725	0.8259	1.1197	0.7693	0.78	1.0574	0.8912
R27	0.8607	1.0515	0.7586	0.7465	1.0347	0.7703	0.751	1.041	0.7366	0.7412	1.0275	0.876
R28	0.7594	0.9692	0.8141	0.7628	0.9743	0.7634	0.7421	0.9769	0.7655	1.168	0.9827	0.7699
R29	0.2430	0.2430	0.2430	0.2454	0.2454	0.2454	0.2465	0.2465	0.2465	0.249	0.249	0.249
sum	18.795	24.444	19.914	18.093	23.597	17.992	18.271	23.860	17.456	18.214	23.234	20.210

**7. References**

[1] M. G. Maleki, R. M. Chabanloo, M. R. Taheri, and H. H. Zeineldin, "Coordination of non - directional overcurrent relays and fuses in active distribution networks considering reverse short - circuit currents of DGs," *IET Generation, Transmission & Distribution*, vol. 15, no. 18, pp. 2539-2553, 2021.

[2] A. S. Noghabi, J. Sadeh, and H. R. Mashhadi, "Considering different network topologies in optimal overcurrent relay coordination using a hybrid GA," *IEEE Transactions on Power Delivery*, vol. 24, no. 4, pp. 1857-1863, 2009.

[3] A. S. Noghabi, H. R. Mashhadi, and J. Sadeh, "Optimal coordination of directional overcurrent relays considering different network topologies

using interval linear programming," *IEEE Transactions on Power Delivery*, vol. 25, no. 3, pp. 1348-1354, 2010.

[4] L. Huchel and H. H. Zeineldin, "Planning the coordination of directional overcurrent relays for distribution systems considering DG," *IEEE Transactions on Smart Grid*, vol. 7, no. 3, pp. 1642-1649, 2015.

[5] T. Amraee, "Coordination of directional overcurrent relays using seeker algorithm," *IEEE Transactions on Power Delivery*, vol. 27, no. 3, pp. 1415-1422, 2012.

[6] M. Lwin, J. Guo, N. B. Dimitrov, and S. Santoso, "Stochastic optimization for discrete overcurrent relay tripping characteristics and coordination," *IEEE Transactions on Smart Grid*, vol. 10, no. 1, pp. 732-740, 2017.

[7] M. Ghotbi-Maleki, R. M. Chabanloo, H. A. Abyaneh, and M. Zamani, "Considering transient short-circuit currents of wind farms in overcurrent relays coordination using binary linear programming," *International Journal of Electrical Power & Energy Systems*, vol. 131, p. 107086, 2021.

[8] E. Purwar, D. Vishwakarma, and S. Singh, "Optimal relay coordination for grid connected variable size DG," *IEEE 6th International Conference on Power Systems (ICPS)*, pp. 1-5, 2016.

[9] A. S. Noghabi, J. Sadeh, and H. R. Mashhadi, "Parameter uncertainty in the optimal coordination of overcurrent relays," *International Transactions on Electrical Energy Systems*, vol. 28, no. 7, p. e2563, 2018.

[10] M. Shabani and A. Karimi, "A robust approach for coordination of directional overcurrent relays in active radial and meshed distribution networks considering uncertainties," *International Transactions on Electrical Energy Systems*, vol. 28, no. 5, p. e2532, 2018.

[11] F. Alasali, N. El - Naily, A. S. Saidi, A. Irtadat, W. Holderbaum, and F. A. Mohamed, "Highly sensitive multifunction protection coordination scheme for improved reliability of power systems with distributed generation (PVs)," *IET Renewable Power Generation*, vol. 17, no. 12, pp. 3025-3048, 2023.

[12] W. El-Khattam and T. S. Sidhu, "Resolving the impact of distributed renewable generation on directional overcurrent relay coordination: a case study," *IET Renewable Power Generation*, vol.3, no.4, pp. 415-425, 2009.

[13] P. Mahat, Z. Chen, B. Bak-Jensen, and C. L. Bak, "A simple adaptive overcurrent protection of distribution systems with distributed generation," *IEEE Transactions on Smart Grid*, vol.2, no.3, pp. 428-437, 2011.

[14] V. A. Papaspiliotopoulos, G. N. Korres, V. A. Kleftakis, and N. D. Hatziaargyriou, "Hardware-in-the-loop design and optimal setting of adaptive protection schemes for distribution systems with distributed generation," *IEEE Transactions on Power Delivery*, vol. 32, no. 1, pp. 393-400, 2015.

[15] E. Purwar, D. Vishwakarma, and S. Singh, "A novel constraints reduction-based optimal relay coordination method considering variable operational status of distribution system with DGs," *IEEE Transactions on Smart Grid*, vol. 10, no. 1, pp. 889-898, 2017.

[16] H. H. Zeineldin, H. M. Sharaf, D. K. Ibrahim, and E. E.-D. A. El-Zahab, "Optimal protection coordination for meshed distribution systems with DG using dual setting directional over-current relays," *IEEE Transactions on Smart Grid*, vol. 6, no. 1, pp. 115-123, 2014.

[17] M. Ojaghi and V. Mohammadi, "Use of clustering to reduce the number of different setting groups for adaptive coordination of overcurrent relays," *IEEE Transactions on Power Delivery*, vol. 33, no. 3, pp. 1204-1212, 2017.

[18] R. M. Chabanloo, M. Safari, and R. G. Roshanagh, "Reducing the scenarios of network topology changes for adaptive coordination of overcurrent relays using hybrid GA-LP," *IET Generation, Transmission & Distribution*, vol. 12, no. 21, pp. 5879-5890, 2018.

[19] M. Ghotbi-Maleki, R. M. Chabanloo, H. H. Zeineldin, and S. M. H. Miangafsheh, "design of setting group-based overcurrent protection scheme for active distribution networks using MILP," *IEEE Transactions on Smart Grid*, vol. 12, no. 2, pp. 1185-1193, 2020.

[20] A. Najjar, H. Kazemi Karegar, and S. Esmailbeigi, "Multi - agent protection scheme for microgrid using deep learning," *IET Renewable Power Generation*, vol. 18, no. 4, pp. 663-678, 2024.

[21] F. Coffele, C. Booth, and A. Dysko, "An adaptive overcurrent protection scheme for distribution networks," *IEEE Transactions on Power Delivery*, vol. 30, no. 2, pp. 561-568, 2014.

[22] S. Shen et al., "An adaptive protection scheme for distribution systems with DGs based on optimized thevenin equivalent parameters estimation," *IEEE Transactions on Power Delivery*, vol. 32, no. 1, pp. 411-419, 2015.

[23] D. S. Kumar, D. Srinivasan, and T. Reindl, "A fast and scalable protection scheme for distribution networks with distributed generation," *IEEE Transactions on Power Delivery*, vol. 31, no. 1, pp. 67-75, 2015.

[24] E. Purwar, S. Singh, and D. N. Vishwakarma, "A robust protection scheme based on hybrid pick-up and optimal hierarchy selection of relays in the variable DGs-distribution system," *IEEE Transactions on Power Delivery*, 2019.

[25] D. S. Kumar, D. Srinivasan, A. Sharma, and T. Reindl, "Adaptive directional overcurrent relaying scheme for meshed distribution networks," *IET Generation, Transmission & Distribution*, vol. 12, no. 13, pp. 3212-3220, 2018.

[26] N. H. Torshizi, H. Najafi, A. S. Noghabi, and J. Sadeh, "An adaptive characteristic for overcurrent relays considering uncertainty in presence of distributed generation," *International Journal of Electrical Power & Energy Systems*, vol. 128, p. 106688, 2021.

[27] V. Chamola and B. Sikdar, "Outage estimation for solar powered cellular base stations," *IEEE International Conference on Communications (ICC)*, pp. 172-177, 2015.

[28] A. K. Kaviani, G. Riahy, and S. M. Kouhsari, "Optimal design of a reliable hydrogen-based stand-alone wind/PV generating system, considering component outages," *Renewable Energy*, vol. 34, no. 11, pp. 2380-2390, 2009.

[29] M. Basu, "Optimal generation scheduling of fixed head hydrothermal system with demand-side management considering uncertainty and outage

of renewable energy sources," *IET Generation, Transmission & Distribution*, vol. 14, no. 20, pp. 4321-4330, 2020.

[30] T. Schossig, "Application of settings and sgs in 1ec 61850," *The Journal of Engineering*, vol. 2018, no. 15, pp. 967-970, 2018.

[31] J. i. Rohn and J. Kreslova, "Linear interval inequalities," *Linear and Multilinear Algebra*, vol. 38, no. 1-2, pp. 79-82, 1994.

[32] F. Mahmood, "Improving the Photovoltaic Model in PowerFactory," Master, Electrical Engineering, KTH, 2017.

[33] *TransmissionCode 2007: Network and System Rules of the German Transmission System Operators*, 2007.

[34] B. Saint, "Update on IEEE P1547. 7-Draft Guide to Conducting Distribution Impact Studies for Distributed Resource Interconnection." *PES T&D 2012. IEEE*, 2012.

[35] A. J. Urdaneta, H. Restrepo, S. Marquez, and J. Sanchez, "Coordination of directional overcurrent relay timing using linear programming," *IEEE Transactions on Power Delivery*, vol. 11, no. 1, pp. 122-129, 1996.

[36] T. K. Barik and V. A. Centeno, "K-medoids clustering of setting groups in directional overcurrent relays for distribution system protection," *IEEE Kansas Power and Energy Conference (KPEC)*, pp. 1-6, 2020.

[37] M. Ghotbi-Maleki, R. M. Chabanloo, M. A. Ebadi, and M. Savaghebi, "Determination of optimal breakpoint set of overcurrent relays using modified depth - first search and mixed - integer linear programming," *IET Generation, Transmission & Distribution*, vol. 14, no. 23, pp. 5607-5616, 2020.

## 8. Appendix

Table A. Short circuit currents for networks with and without DGs

Relay	IEEE 30-bus		8-bus standard system		
	without DGs	with DGs	Relay	without PVs	with PVs
R1	3.408	3.661	R1	1.498	1.537
R2	3.491	4.188	R2	2.763	2.803
R3	1.978	2.311	R3	1.733	1.750
R4	4.877	5.469	R4	1.001	1.073
R5	5.100	5.553	R5	1.001	1.081
R6	5.089	5.738	R6	2.628	2.699
R7	1.942	2.586	R7	2.254	2.319
R8	3.503	4.283	R8	2.628	2.690
R9	3.204	4.156	R9	1.076	1.131
R10	3.575	4.143	R10	1.819	1.899
R11	3.087	3.305	R11	1.819	1.827
R12	4.327	4.981	R12	2.763	2.782
R13	3.997	4.969	R13	1.388	1.418
R14	5.231	5.925	R14	2.254	2.303
R15	2.889	3.203			
R16	2.195	2.594			
R17	1.117	1.162			
R18	3.087	3.305			
R19	2.667	3.620			
R20	2.161	2.355			
R21	3.649	4.027			
R22	1.073	1.295			
R23	1.359	1.817			
R24	2.061	2.394			
R25	2.664	2.828			
R26	1.907	2.322			
R27	2.887	3.094			
R28	1.163	1.199			
R29	0.776	0.807			